UDC 622.841:622.51.2 DOI: https://doi.org/10.15407/geotm2025.174.058

SEEPAGE OF GROUNDWATER TOWARDS A TUNNEL EXCAVATED IN FRACTURED ROCK

[1]Krukovska V., [1]Krukovskyi O., [2]Vynohradov Y.

[1]M.S. Poliakov Institute of Geotechnical Mechanics of the National Academy of Sciences of Ukraine
[2]Branch for Physics of Mining Processes of the M.S. Poliakov Institute of Geotechnical Mechanics of the NAS of Ukraine

Abstract. Groundwater represents one of the key factors affecting the stability and safety of tunnels, particularly during the early stages of construction, when temporary support and lining have not yet been installed. Delays at this stage may lead to increased rock mass deformation, widening of the permeable zone, opening of fractures, and significant groundwater inflows, potentially resulting in structural hazards and adverse environmental impacts. To address these challenges, this study develops a finite element model to investigate the coupled processes of rock mass deformation and groundwater flow into a tunnel excavated in hard rocks with different degrees of disturbance.

The results show that intact rock masses at a depth of 50 m undergo purely elastic deformations, with negligible tunnel wall displacements and minimal changes in permeability, indicating a stable geological environment. In contrast, disturbed zones exhibit significant hydro-mechanical coupling effects. With increasing disturbance, rock strength decreases, the relative principal stress differential is reduced, and susceptibility to brittle or plastic failure rises. Intense fracturing causes block separation, while saturated kaolinized zones undergo plastic deformation due to clay softening. These conditions result in pronounced tunnel wall displacements, enhanced permeability near the excavation boundary, and, in highly fractured rocks, the development of a wide depression zone in pore pressure. Such alterations in the hydrogeological regime can lower groundwater levels, impact aquifers and natural springs, and trigger soil settlement due to loss of pore pressure.

The findings emphasize the importance of minimizing the time between excavation and support installation, especially when tunneling through disturbed geological zones. Since unpredicted fault zones and fracture networks may not be fully identified during site investigation, tunnel support design should include adaptive reinforcement strategies to ensure safety and environmental protection. The study provides novel insights into the short-term interaction between rock mass disturbance and groundwater flow, contributing to improved risk assessment and design optimization in underground construction.

Keywords: tunnel, fractured rock, groundwater flow, hydraulic influence of unsupported tunnel, numerical simulation.

1. Introduction

The increasing utilization of underground space for transportation systems and other industrial and public needs has necessitated more detailed investigations into the problems associated with ensuring the long-term stability and operational safety of such structures under various geological conditions.

Groundwater is one of the key factors threatening stability and safety already during construction, and therefore groundwater control is of great importance [1–3]. Reliable prediction of groundwater inflow can lead to significant cost savings for future tunneling projects, as well as prevent negative impacts on the environment and surface infrastructure [3–5]. Notable examples of hazards related to the interaction between a water-bearing environment and an underground structure include the Romeriksporten railway tunnel in Norway, which caused a lowering of the groundwater table and surface subsidence [6], and the Milan Metro tunnel network in Italy, which faces a flooding threat due to a rising groundwater table [7].

The study of fluid flow through hard rock masses remains challenging, as the process depends on the hydraulic properties of complexly structured rock masses, which vary under stress changes [8, 9]. The main groundwater inflow paths during tunnel

Received: 20.07.2025 Accepted: 15.09.2025 Available online: 19.09.2025

excavation are: diffuse inflow (originating from a network of distributed fractures along the tunnel) and concentrated inflow along certain tectonic faults [10]. Hydraulic conductivity or permeability is the most complex and important factor in estimating tunnel groundwater inflow [11], with an extremely wide variability exceeding ten orders of magnitude (10^{0}–10^{-10} m/s) [10], as shown in Table 1.

Table 1 – Empirical relationships between permeability determined from testing and rock mass condition [10]

Hydraulic conductivity K, m/s	Rock mass condition and hydraulic resistance
$< 10^{-8}$	Compressed rock mass with numerous tight, closed fractures – impervious rock
$10^{-8} – 3 \cdot 10^{-6}$	Unloaded rock mass with numerous closed and open fractures – diffuse permeability
$> 3 \cdot 10^{-6}$	Unloaded to loosened rock mass with open and large fractures – high, continuous permeability
$> 10^{-7}$	High groundwater inflows along the tunnel
$> 10^{-5}$	Inflows can cause severe problems during works and for the surrounding environment

Detailed knowledge of fault properties enables the most accurate assessment of hydraulic flow in a rock mass hosting a tunnel [10, 12]. However, geological conditions may vary drastically. Construction of the Laliki Tunnel in Poland, near the Polish–Slovak border, demonstrated that fracture and fault patterns, as well as other hydraulic characteristics, changed almost with every advance of the tunnel face, making prediction and assessment ineffective [13]. A similar situation was observed during construction of the Dnipro Metro. Therefore, it is impossible to fully reproduce the geological structure of the rock mass with all its property variations when calculating groundwater inflows.

Ensuring tunnel stability is equally complex. At shallow depths, where tunnels are usually constructed, the rock mass is blocky and fractured. Stability problems here are related to wedge falls from the crown and sidewalls of the tunnel under gravity [14]. Depending on the degree of rock disturbance – ranging from intact continuum to highly fractured mass – stabilization measures vary from no support to rockbolts, steel sets, reinforced concrete lining, and various combinations thereof [14]. Cement grouting is also frequently applied for tunnel support [15, 16].

The choice of support is crucial for ensuring tunnel stability and maintaining the host rock in an undisturbed, impermeable state for gas and water [17–19]. The influence of different types of support on underground structure stability was investigated by numerous researchers worldwide [2, 13, 14, 20–25]. The studies addressed the effect of rockbolt parameters on the formation of a strong rock–bolt structure [20], rockbolt behavior in block-structured rock masses [21], the influence of rockbolt installation density on surrounding rock deformation and plastic zone radius [22], rock mass reinforcement using grouted rockbolts [23, 24], the influence of the grouting ring thickness on tunnel groundwater inflow [2], and the effect of steel corrosion on the long-term performance of metallic support under increased groundwater inflows [25].

Tunnel support is installed sequentially according to geological and technological conditions at different construction stages: rock excavation at the face, installation of initial support, and installation of final lining. Due to unforeseen circumstances, including wartime conditions, significant delays may occur at any preparatory stage – as seen in the construction of the second line of the Dnipro Metro, where the first construction stage has already lasted several years [26]. Delays in installing initial or final support contribute to further deformation of the rock mass, expansion of the permeable zone, and opening of individual fractures and faults, which stimulate groundwater inflows with destructive consequences.

Early investigation of these processes helps prevent environmental problems, such as long-term impacts on the groundwater table, aquifers, and water quality [14]. In this context, the aim of this study is to investigate groundwater seepage into a tunnel excavated in fractured rock during the first construction stage, in the period between rock excavation and installation of the initial support.

To achieve this aim, the following objectives were set:

- to develop a mathematical and numerical model of coupled processes of rock deformation and groundwater seepage into an underground tunnel excavated in fractured rock;
- to investigate the time evolution of rock deformation and groundwater seepage into an unsupported tunnel constructed outside fault zones;
- to examine the influence of rock mass disturbance on rock deformation and groundwater seepage into an unsupported tunnel.

2. Methods

The coupled processes of rock mass deformation and groundwater seepage are described by the following system of equations [17]:

$$c_g \frac{\partial u_i}{\partial t} = \sigma_{ij,j} + X_i(t) + P_i(t);$$

$$\mathrm{S}\frac{\partial p}{\partial t} = K\left(\frac{\partial^2 p}{\partial x^2} + \frac{\partial^2 p}{\partial y^2}\right);$$

where c_g – damping coefficient, kg/(m³·s); t – time, s; u_i – displacement, m; $\sigma_{ij,j}$ – derivatives of stress tensor components with respect to x, y, Pa/m; $X_i(t)$ – projections of external forces acting on a unit volume of solid, N/m³; $P_i(t)$ – projections of forces caused by water pressure in the fracture–pore space, N/m³; S – specific storage, m^{-1}, $S = \rho g(m \cdot \beta_w + \beta_r)$; ρ – water density, kg/m³; g – gravitational acceleration, m/s²; m – rock porosity, %; β_w – water compressibility, Pa^{-1}; β_r – rock compressibility, Pa^{-1}; p – water pressure, Pa; K – hydraulic conductivity, m/s.

The problem is solved in an elastoplastic formulation. The Mohr–Coulomb failure criterion is used to describe the transition of rock into a disturbed state [27, 28].

The initial and boundary conditions for the problem are:

$$\sigma_{yy}\big|_{t=0} = \gamma H; \quad \sigma_{xx}\big|_{t=0} = \lambda\gamma H; \quad p\big|_{t=0} = (h + y_0 - y)\rho g;$$
$$u_x\big|_{\Omega_1} = 0; \quad u_y\big|_{\Omega_2} = 0; \quad p\big|_{\Omega_3} = 0.1 \text{ МПа},$$

where γ – average unit weight of overlying rocks, N/m³; H – tunnel depth, m; λ – lateral rock pressure coefficient; h – piezometric head, m; y_0 – coordinate of the central point of the FEM mesh, m; Ω_1 – vertical boundaries of the external contour; Ω_2 – horizontal boundaries of the internal contour; Ω_3 – tunnel contour.

To assess the stress state, the following dimensionless parameters are used: the relative principal stress differential $Q^* = (\sigma_1 - \sigma_3)/\gamma H$, and unloading index $P^* = \sigma_3/\gamma H$.

Hydraulic conductivity $K = k\rho g/\mu$, where k – permeability coefficient, m²; μ – dynamic viscosity of water, Pa·s. Rock mass permeability coefficients k is determined both by geological factors [29] and by tunneling and support installation methods. Excavation causes redistribution of the initial stress field, leading to the formation of new fracture systems in the rock mass. The initial permeability field k_0 is superimposed with the technological permeability field k_{tech}, which depends on the stress tensor components [25]:

$$k = k_0 + k_{\text{tech}}\left(t,\ Q^*,\ P^*\right).$$

$$k_{\text{tech}} = \begin{cases} 0, \text{ if } Q^* < 0.4; P^* > 0.4; \\ A, \text{ if } 0.4 < Q^* < 0.6;\ P^* < 0.4; \\ e^{0.26Q^* - 4.65} + A, \text{ if } 0.6 < Q^* < 1.0;\ P^* < 0.4; \\ k_{\max}, \text{ if } Q^* > 1.0;\ \ P^* < 0.4, \end{cases}$$

where $A = k_{\max}\cdot(1\text{-}2.5\cdot P^*)$; $k_{\max}$ – permeability of completely fractured rock, m².

The strength and hydraulic conductivity K_0 of strong rocks (such as granite) are significantly affected by fracturing: fractures reduce strength and increase hydraulic conductivity [30], even if the granite material itself is very strong. For example, along the Dnipro Metro tunnel alignment, zones of non-uniformly fractured granite, strongly and intensely fractured granite, crushed and mylonitized zones, and intensely kaolinized zones occur (Figure 1).

Non-uniformly fractured granite, where most of the rock mass is strong but contains isolated or poorly cemented fractures, can still bear loads but requires caution. Strongly and intensely fractured granite is typically found in fault zones, where it loses monolithic structure, becomes weak (like compacted gravel), and exhibits high permeability. The strength and filtration properties of various disturbed zones are shown in Table 2.

Zones of crushing and mylonitization are characterized by intense tectonic shearing and pressure, which grind the rock into a fine-grained mass, but some foliation may remain and residual strength can be preserved. Mylonite is a strongly deformed, crushed rock. Compressive strength: strongly mylonitized rocks – $\sigma_c \approx$ 5–10 MPa;

weakly mylonitized – up to 30–50 MPa. Strength is much lower than that of the original rock but generally higher than in kaolinized zones, since clay minerals are absent. Hydraulic conductivity varies widely depending on fracture density and compaction: $K_0 \approx 10^{-10} – 10^{-7}$ m/s. Highly fractured or loosened mylonite approaches $K_0 \approx 10^{-10}–10^{-7}$ m/s; compacted mylonite is nearly impermeable (Table 2).

– non-uniformly fractured rocks;
– strongly and intensely fractured rocks;
– zones of crushing and mylonitization;
– zones of intense kaolinization.

Figure 1 – Disturbed zones along the Dnipro Metro tunnel alignment

Table 2 – Strength and hydraulic properties of granite in disturbed zones

Zone type	Main mineral	Compressive strength σ_c, MPa	Initial hydraulic conductivity K_0, m/s	Properties
Intact rock	Granite	100–250	$10^{-11}–10^{-9}$	High strength, almost impermeable
Non-uniformly fractured	Granite	30–80	$10^{-8}–10^{-6}$	Partially strong, isolated weak zones; permeability via individual fractures
Strongly fractured	Granite	5–30	$10^{-6}–10^{-4}$	Reduced bearing capacity, noticeable permeability
Intensely fractured	Granite	1–10	$10^{-4}–10^{-2}$	Easily disintegrates, loses monolithic structure, high permeability
Mylonitized zone	Quartz, micro-crystalline minerals	5–30	10^{-7} (fractured) 10^{-10} (compacted)	Residual strength possible; permeability variable
Kaolinized zone	Kaolinite (clay)	0.5–5	$10^{-9}–10^{-7}$ $10^{-8}–10^{-6}$ (wet)	Unstable when wet; low strength; permeability fracture-dependent

Zones of intense kaolinization exhibit mechanical and hydraulic properties that differ greatly from intact rock. Strongly kaolinized rock has compressive strength $\sigma_c \approx 0.5$–5 MPa (sometimes < 0.5 MPa if almost pure kaolinite). For comparison, intact granite has $\sigma_c \approx 100$–250 MPa. Strength drops sharply due to the decomposition of cementing minerals and formation of clay aggregates that swell when wetted and disintegrate under load. Hydraulic conductivity: dry $K_0 \approx 10^{-9}$–10^{-7} m/s; wet (after structural collapse) $K_0 \approx 10^{-8}$–10^{-6} m/s. Although kaolinite has low intrinsic permeability, fractures or macroporosity may temporarily increase flow rates. Such zones are unstable, easily soften, have low strength, and can cause significant problems during excavation, drilling, or underground construction (Table 2).

Approximate relationships between strength and initial conductivity K_0 of strong rocks versus rock mass fracturing are shown in Figure 2.

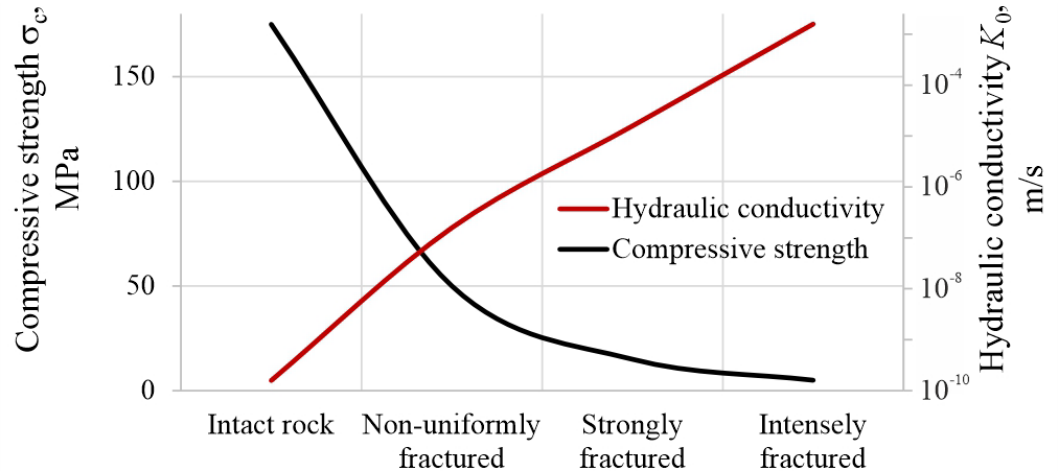

Figure 2 – Relationship between strength and initial hydraulic conductivity of strong rocks and rock mass fracturing

In this study, the tunnel cross-section is 6.1 m high and 6.0 m wide, at a depth of 50 m. The groundwater table is located 3 m below the surface. The mechanical and hydraulic properties of the rock used in the calculations are listed in Table 3.

Table 3 – Strength and hydraulic properties of rock in disturbed zones

Zone	Rock mass disturbance	Compressive strength σ_c, MPa	Modulus of elasticity E, MPa	Cohesion C, MPa	Hydraulic conductivity K_0, m/s
No. 1	Intact granite	100	12000	30	10^{-10}
No. 2	Non-uniformly fractured	50	7500	10	10^{-7}
No. 3	Strongly fractured	10	5000	3	10^{-4}
No. 4	Intensely fractured	1	2500	0.3	10^{-2}
No. 5	Mylonitized, crushed	5	2500	1.5	10^{-7}
No. 6	Kaolinized (wet)	0.5	2000	0.28	10^{-6}

The finite element method (FEM) was used to solve the problem [31, 32]. At each time step i ($\Delta t = 3$ h), the influence of the stress field on the formation of the seepage zone and the effect of changes in water pressure on the rock stress state were taken into account.

It should be noted that although FEM considers a continuum rather than a discrete rock mass, it allows approximation of the hydraulic effect of fluid flow through rock fractures by using hydraulic conductivity for the rock mass. This approach has been widely applied to groundwater flow problems in tunneling [14]. Discrete element analysis is sometimes difficult to implement because it requires detailed input parameters, such as joint positions, joint spacing, joint connectivity, joint hydraulic apertures, and normal and shear stiffness. Without adequate input data, discrete element analysis results are unreliable [14]. Moreover, FEM has been repeatedly used to obtain useful and reliable results in assessing tunnel stability for excavations in both continuous and discrete rock masses [33].

3. Time evolution of deformation and groundwater flow

The time evolution of deformation and groundwater flow processes was studied over an 8-day period, during which these processes largely stabilise and transit into a quasi-steady regime. Figure 3 shows the distributions of geomechanical and seepage parameters for case No. 1 (intact granite) at different time moments.

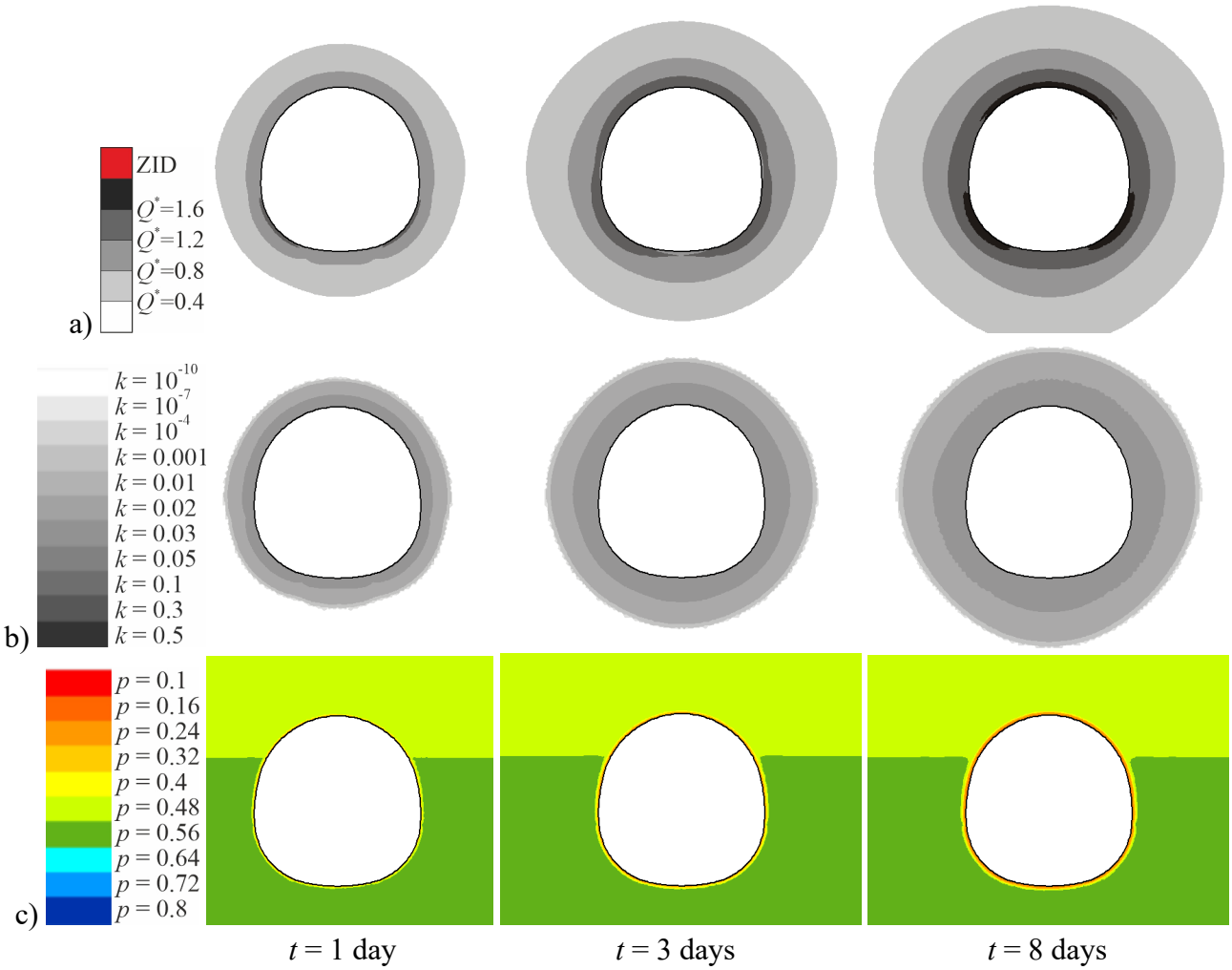

a) parameter Q^*; b) hydraulic conductivity K, m/s; c) water pressure p, MPa.

Figure 3 – Distributions of parameters at t = 1 day; t = 3 days, and t = 8 days

An intact rock mass at a depth of 50 m is subjected to loading from the overburden and is under a pressure of 1.25 MPa. Existing isolated fractures are tightly closed, and hydraulic conductivity is practically absent. During tunnel excavation, the confining stress at the tunnel boundary is removed, and the compressed rock mass begins to unload. The relative principal stress differential Q^* in the near-contour zone increases with time (Figure 3a), reaching values $Q^* > 1.6$ in some sectors by day 8. The locations of these peaks are controlled by the irregular circular shape of the excavation.

Figure 4a shows that the depth of the zone with elevated differential stress at $t = 1$ day is 5 m, gradually propagating deeper into the rock mass over time. Strong, intact rock with high compressive strength deforms elastically. At $t = 1$ day, the displacement of the central point in the tunnel crown is $u = 0.016$ mm, increasing to $u = 0{,}032$ mm at $t = 8$ days (Figure 4b). This is a very small value, allowing the host rock to be confidently classified as stable.

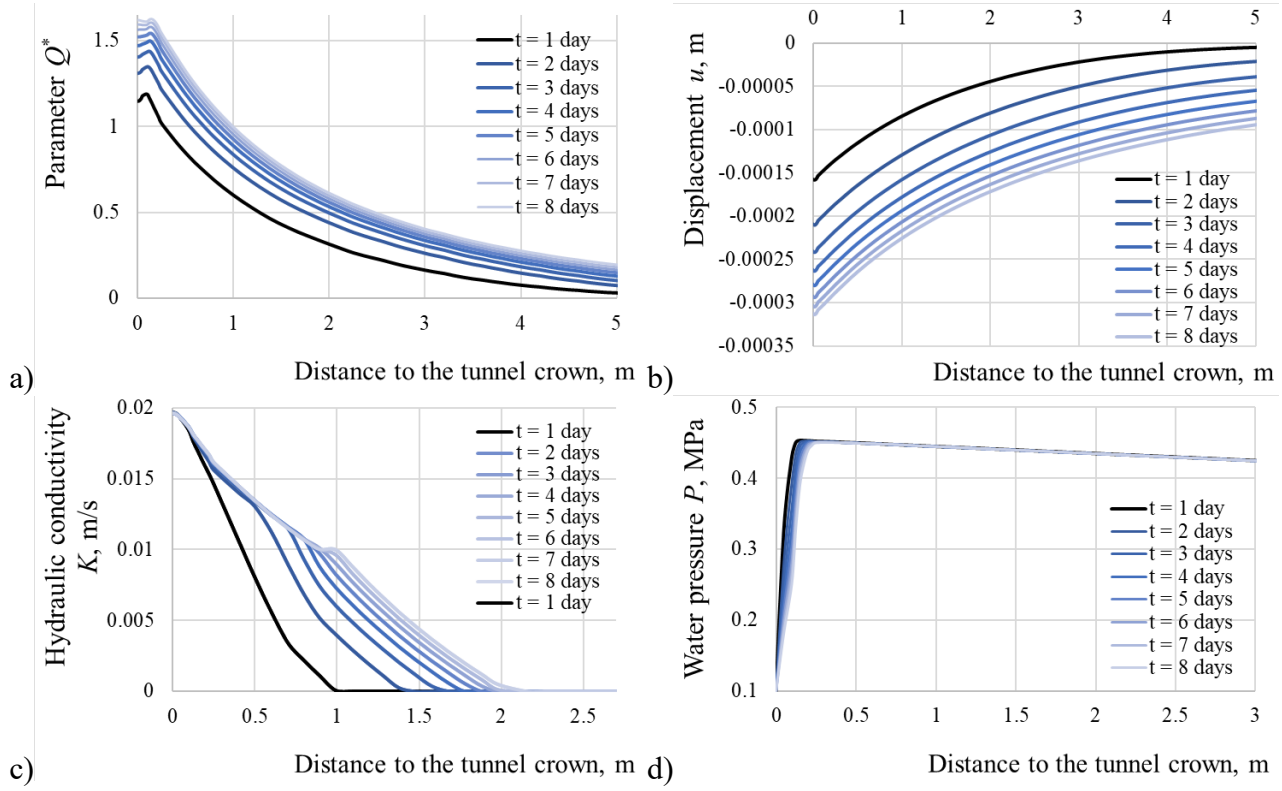

a) parameter Q^*; b) displacement of the central crown point; c) hydraulic conductivity of crown rock; d) water pressure.

Figure 4 – Variations of deformation and seepage parameters in the tunnel crown along the vertical line passing through its centre

During unloading, previously closed fractures open, and the permeability of near-contour rock increases (Figures 3b, 4c). However, it remains too low to sustain significant groundwater flow. The water pressure around the excavation changes only minimally over the analysed period (Figures 3c, 4d).

4. Influence of rock mass disturbance on deformation and groundwater flow

The deformation and groundwater flow parameters were further calculated for disturbed zones: non-uniformly fractured, strongly fractured, and intensely fractured rock, as well as for the crushed mylonitised zone and the kaolinised zone in a wet state (Table 3). The results at $t = 8$ days are shown in Figures 5 and 6.

The average value of Q^* within a 12×12 m area around the tunnel increases with time in all six analysed cases (Figure 6a). Figure 5 shows that, as rock strength decreases, both the area of elevated differential stress ($Q^* > 0.4$) around the tunnel and the values of Q^* within that area decrease. In non-uniformly fractured rock, Q^* exceeds 1.2 near the tunnel boundary (Figure 5a), whereas in strongly fractured rock $Q^* < 1.2$ (Figure 5b), and in intensely fractured rock $Q^* < 0.55$ (Figure 5c).

Weaker rock cannot sustain high differential stress and begins to fail; thus, in cases No. 4 (Figure 5c) and No. 6 (Figure 5e) a 1.2–1.5 m-thick near-contour layer undergoes inelastic deformation. Intensely fractured granite in case No. 4 fails in a brittle manner through block separation, whereas wet kaolinite in case No. 6 deforms plastically.

Accordingly, the largest normal displacements of the tunnel contour occur in intensely fractured rock (No. 4) and in the kaolinised zone (No. 6), where inelastic deformation zones are present (Figure 6b). Interestingly, the contour displacement is quite non-uniform: maximum contour displacements occur at the bottom (node 100) and at the sidewalls (nodes 47 and 153), due to the large radius of curvature and near-linear geometry of the surface in these areas.

In the second column of Figure 5, the hydraulic conductivity distributions on day 8 after tunnel face advance are shown for cases No. 2–No. 6. The difference in initial rock mass permeability and its significant increase in the immediate vicinity of the tunnel contour with deterioration of rock quality is clearly visible. The average permeability around the tunnel increases with time (Figure 6c) and reaches the highest values in intensely fractured rock with a large inelastic zone.

The permeability level controls the intensity of seepage; thus, in case No. 1, the pore water pressure in the fracture network around the tunnel changes little over time (Figure 3c). At $t = 8$ days, in non-uniformly fractured (No. 2), strongly fractured (No. 3) rock, and in the mylonitised zone (No. 5), pore water pressure is noticeably lower in the near-contour zone. In intensely fractured granite (No. 4) and in the kaolinised zone (No. 6), a wide area develops around the tunnel where $p < 0.4$p, which is significantly below the hydrostatic pressure at this depth.

Looking at the last column in Figure 5d, which shows water pressure distributions at a smaller scale, it can be seen that in case No. 4, unlike the others, a local pressure depression develops: the isobars $p = 0.32$, $p = 0.4$, $p = 0.56$, and $p = 0.64$ are bent toward the tunnel. Thus, under conditions of high rock mass permeability, as in case No. 4, there is a significant hydraulic influence of an unsupported tunnel on the natural groundwater regime, with changes in both pressure and flow direction.

The formation of a local, limited-size depression cone by day 8 after tunnel face advance may subsequently lead to a lowering of the groundwater table, potentially

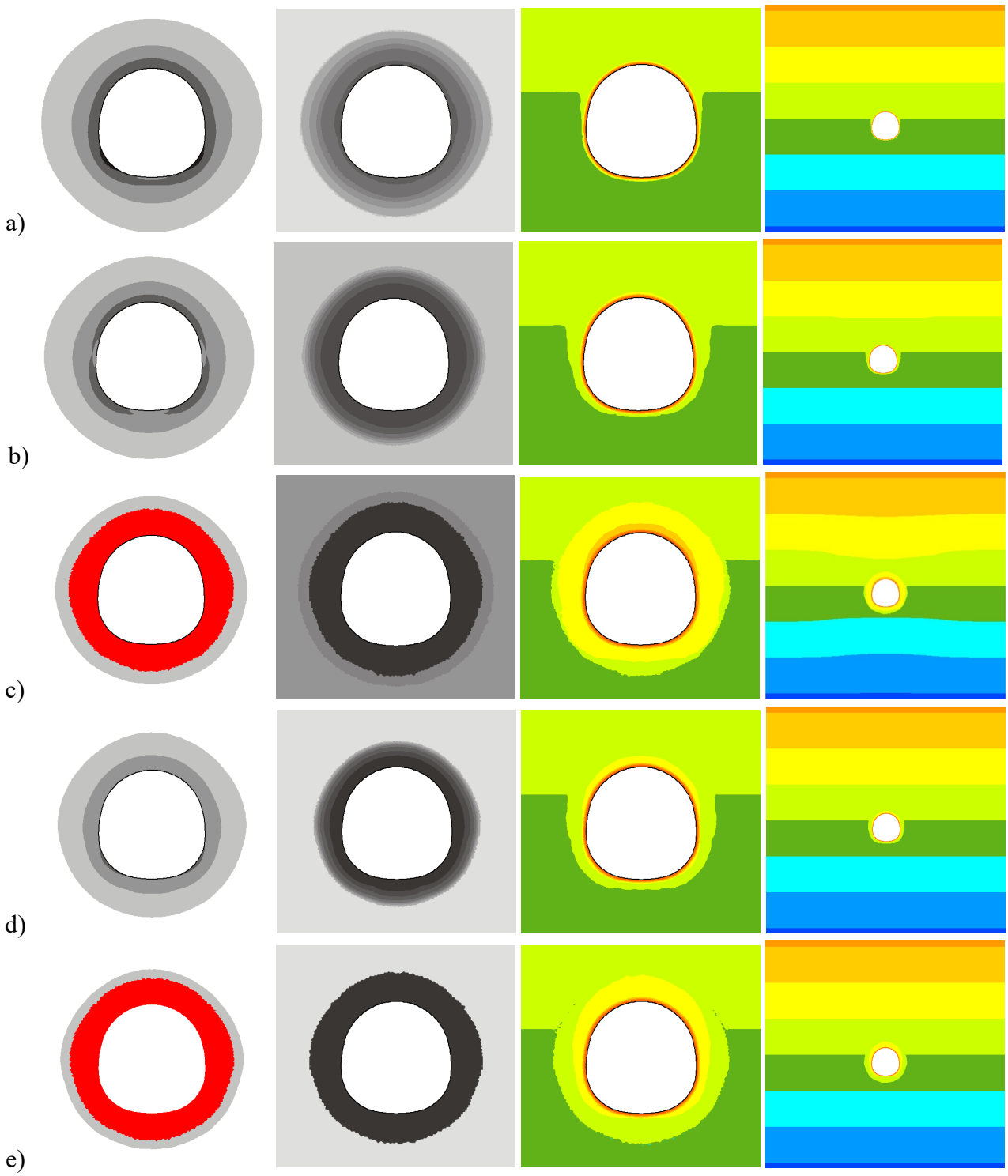

a) non-uniformly fractured rock (No. 2); b) strongly fractured rock (No. 3); c) intensely fractured rock (No. 4); d) crushed mylonitised zone (No. 5); e) kaolinised zone in a wet state (No. 6).

Figure 5 – Distributions of parameter Q^* and zones of inelastic deformations; filtration coefficients k; water pressure p around the tunnel and water pressure p at a smaller scale at t = 8 days

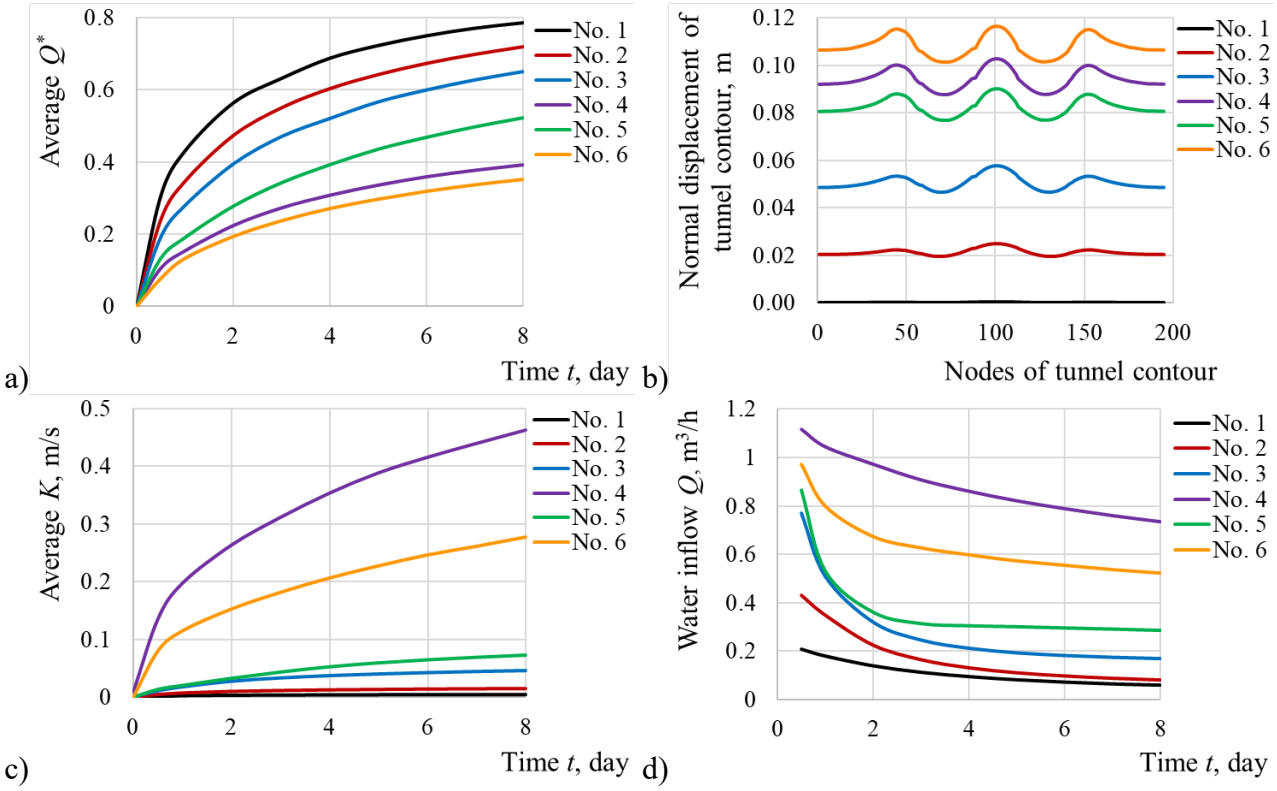

a) average Q^* in a 12×12 m area; b) normal displacement of tunnel contour (nodes 0 and 200 – crown, node 100 – bottom) at t = 8 days; c) average conductivity k in a 12×12 m area; d) groundwater inflow into the tunnel.

Figure 6 – Variations of deformation and seepage parameters

affecting water intakes, natural springs, soil drainage, and ground settlement due to pore pressure loss.

5. Conclusions

Groundwater is one of the key factors threatening tunnel stability and safety already at the construction stage. Delays in installing support and sealing the tunnel lining, which may occur under unforeseen circumstances, represent a particular hazard. This study addressed groundwater inflow to tunnels at the initial construction stage – in the period between excavation and installation of support. For this purpose, a mathematical and numerical model was developed to analyze the coupled processes of rock mass deformation and water filtration in rock masses of varying degrees of disturbance.

The main findings of the study are as follows.

1) For intact rock masses with high compressive strength, tunnel wall displacements remain minimal, the rock deforms elastically, and the permeability of the near-tunnel zone increases only slightly, insufficient to produce significant groundwater flow.

2) With increasing disturbance of the rock mass, its strength decreases, which reduces the relative principal stress differential and increases susceptibility to failure. In intensely fractured zones, brittle block separation occurs, whereas in kaolinized zones,

plastic failure develops due to saturated kaolinite. These cases also exhibit the largest tunnel wall displacements.

3) Increased permeability of disturbed zones intensifies groundwater flow: pore water pressure decreases significantly in near-tunnel zones, and in intensely fractured rock a wide depression zone is formed, altering the natural hydrogeological regime. This may lead to groundwater level decline, affect water intakes and natural springs, and cause soil desiccation and settlement due to pore pressure reduction.

The results confirm that minimizing the time interval between excavation and installation of temporary support and sealing is crucial, particularly in intensely disturbed zones. Furthermore, since not all geological discontinuities along the tunnel alignment can be predicted in advance, tunnel support design should incorporate the possibility of local reinforcement when encountering unforeseen geological structures.

These results provide new insights into the short-term interaction between rock mass disturbance and groundwater flow and can assist in improving the design and risk management of tunnels constructed in fractured rock environments.

Conflict of interest

Authors state no conflict of interest.

REFERENCES

1. Fang, Y., Guo, J., Grasmick, J. and Mooney, M. (2016), "The effect of external water pressure on the liner behavior of large cross-section tunnels", *Tunnelling and Underground Space Technology*, no. 60, pp. 80–95. http://dx.doi.org/10.1016/j.tust.2016.07.009

2. Zhang, G.-H., Jiao, Y.-Y. and Wang, H. (2014), "Outstanding issues in excavation of deep and long rock tunnels: a case study", *Canadian Geotechnical Journal*, no. 51, pp. 984–994. https://doi.org/10.1139/cgj-2013-0087

3. Holmøy, K.H. and Nilsen, B. (2014), "Significance of geological parameters for predicting water inflow in hard rock tunnels", *Rock Mechanics and Rock Engineering*, no. 47, pp. 853–868. https://doi.org/10.1007/s00603-013-0384-9

4. Preisig, G., Dematteis, A., Torri, R., Monin, N., Milnes, E. and Perrochet, P. (2014), "Modelling discharge rates and ground settlement induced by tunnel excavation", *Rock Mechanics and Rock Engineering*, no. 47, pp. 869–884. http://dx.doi.org/10.1007/s00603-012-0357-4

5. Dammyr, Ø., Nilsen, B., Thuro, K. and Grøndal, J. (2014), "Possible concepts for waterproofing of Norwegian TBM Railway Tunnels", *Rock Mechanics and Rock Engineering*, no. 47, pp. 985–1002. http://dx.doi.org/10.1007/s00603-013-0388-5

6. Beitnes, A. (2005), "Lessons to be learned from Romeriksporten", *Tunnels and Tunnelling International*, no.37(6), pp. 36–38. https://trid.trb.org/View/761838

7. Colombo, L., Gattinoni, P. and Scesi, L. (2018), "Stochastic modelling of groundwater flow for hazard assessment along the underground infrastructures in Milan (northern Italy)", *Tunnelling and Underground Space Technology*, no. 79, pp. 110–120. https://doi.org/10.1016/j.tust.2018.05.007

8. Pihulevskyi, P.G., Anisimova, L.B., Tiapkin, O.K. and Yemelianenko, T.M. (2022), "Investigation of the hydrodynamics of man-made water by remote methods (on the example of Southern Kryvbas)", *Geo-Technical Mechanics*, no. 163, pp. 165-173. https://doi.org/10.15407/geotm2022.163.165

9. Wang, Z., Bi, L., Kwon, S., Qiao, L. and Li, W. (2020), "The effects of hydro-mechanical coupling in fractured rock mass on groundwater inflow into underground openings", *Tunnelling and Underground Space Technology*, no. 103, 103489. https://doi.org/10.1016/j.tust.2020.103489

10. Coli, M. and Pinzani, A. (2014), "Tunnelling and hydrogeological issues: A short review of the current state of the art", *Rock Mechanics and Rock Engineering*, no. 47, pp. 839–851. https://doi.org/10.1007/s00603-012-0319-x

11. Zarei, H.R., Uromeihy, A. and Sharifzadeh, M. (2013), "A new tunnel inflow classification (TIC) system through sedimentary rock masses", *Tunnelling and underground space technology*, no. 34, pp. 1-12. http://dx.doi.org/10.1016/j.tust.2012.09.005

12. Sweetenham, M.G., Maxwell, R.M. and Santi, P.M. (2017), "Assessing the timing and magnitude of precipitation-induced seepage into tunnels bored through fractured rock", *Tunnelling and Underground Space Technology*, no. 65, pp. 62–75. http://dx.doi.org/10.1016/j.tust.2017.02.003

13. Majcherczyk, T., Niedbalski, Z. and Kowalski, M. (2012), "3d numerical modeling of road tunnel stability – the Laliki project", *Archives of Mining Sciences*, no. 57(1), pp. 61–78. http://dx.doi.org/10.2478/v10267-012-0005-6

14. U.S. Department of Transportation Publication (2009), *No. FHWA-NHI-10-034: Technical Manual for Design and Construction of Road Tunnels — Civil Elements*, Federal Highway Administration, Washington, US. available at: https://www.fhwa.dot.gov/bridge/tunnel/pubs/nhi09010/tunnel_manual.pdf (Accessed 14 July 2025)

15. Shin, H.-S. (2008), "Tunnelling project in difficult geological conditions in Korea", *the 42nd U.S. Rock Mechanics Symposium and 2nd U.S.-Canada Rock Mechanics Symposium*, San Francisco, U.S., ARMA 08-103. available at: https://onepetro.org/ARMAUSRMS/proceedings-abstract/ARMA08/ARMA08/118388 (Accessed 14 July 2025)

16. Spreng, S.P., McRae, M.T., Nolting, R.M., Desai, H. (2008), "Tunnel Design and Construction in a Franciscan Melange", *the 42nd U.S. Rock Mechanics Symposium and 2nd U.S.-Canada Rock Mechanics Symposium*, San Francisco, U.S., ARMA 08-328. https://onepetro.org/ARMAUSRMS/proceedings-abstract/ARMA08/ARMA08/119248

17. Krukovska, V.V. and Vynohradov, Y.O. (2019), "Water stability influence of host rocks on the process of water filtration into mine working with frame and roof-bolting support", *Geo-Technical Mechanics*, no. 147, pp. 54–61. https://doi.org/10.1051/e3sconf/201910900041

18. Krukovska, V.V. and Vynohradov, Y.O. (2021), "Formation of gas- and water-impermeable area in a mine working roof with injection bolts", *Geo-Technical Mechanics*, no. 156, pp. 3–11. https://doi.org/10.15407/geotm2021.156.003

19. Krukovska, V.V., Krukovskyi, O.P. and Demchenko, S.V. (2023), "Numerical analysis of the possibility of noxious gases infiltration into a shelter located in a gas-bearing coal-rock mass", *Geo-Technical Mechanics*, no. 166, pp. 95–108. https://doi.org/10.15407/geotm2023.166.095

20. Krukovskyi, O.P. (2020), "Formation of elements of the bolting structure for mine workings", *Geo-Technical Mechanics*, no. 151, pp. 27–62. https://doi.org//10.15407/geotm2020.151.027

21. Krukovskyi, O., Krukovska, V., Demin, V., Bulich, Yu. and Khvorostian, V. (2024), "Numerical study of the interaction of rock bolts with the block-structured rock mass", *Geo-Technical Mechanics*, no. 168, pp. 152–163. https://doi.org/10.15407/geotm2024.168.152

22. Ma, W., Zhou, X., Song, Y., Zhang, S., Wu, T., Zhang, J. and Liu, Y. (2024), "Semi-analytical study for cylindrical tunnels reinforced by bolt-grouting in elastic–brittle–plastic surrounding rock considering nonlinear seepage", *Rock Mechanics and Rock Engineering*, no. 57, pp. 3281–3314. https://doi.org/10.1007/s00603-023-03747-9

23. Krukovskyi, O., Krukovska, V., Kurnosov, S., Demin, V., Korobchenko, V. and Zerkal, V. (2023), "The use of steel and injection rock bolts to support mine workings when crossing tectonic faults", *IOP Conference Series: Earth and Environmental Science*, no. 1156, 012024. https://doi.org/10.1088/1755-1315/1156/1/012024

24. Slashchov, I., Slashchova, O., Seleznov, A., Shmyglov, V., Kryvenko, Ye. and Brizheniuk, V. (2024), "Justification of the parameters of injection rock hardening zones around mining workings and buried structures of critical infrastructure", *Geo-Technical Mechanics*, no. 170, pp. 165-180. https://doi.org/10.15407/geotm2024.170.165

25. Krukovska, V., Krukovskyi, O., Vynohradov, Y., Demin, V. and Holovin, M. (2025), "Numerical simulation of aggressive mine water effect on the long-term serviceability of metal support in mine workings", *IOP Conference Series: Earth and Environmental Science*, no. 1491(1), 012058. https://doi.org/10.1088/1755-1315/1491/1/012058

26. Vidomo (2025), "Budivnytstvo metro u Dnipri: v shakhtakh vidkachuiut vodu i obrobliaiut tuneli" [Construction of the Dnipro metro: water is being pumped out of the mines and tunnels are being processed], available at: https://vidomo.media/ukr/city-life/1740991041-budivnitstvo-metro-u-dnipri-v-shahtah-vidkachuyut-vodu-i-obroblyayut-tuneli-foto (Accessed 14 July 2025)

27. Labuz, J.F. and Zang, A. (2012), "Mohr-Coulomb Failure Criterion", *Rock Mechanics and Rock Engineering*, no. 45, pp. 975–979. https://doi.org/10.1007/s00603-012-0281-7

28. Jiang, H. (2015), "Failure criteria for cohesive-frictional materials based on Mohr-Coulomb failure function", *International Journal for Numerical and Analytical Methods in Geomechanics*, no. 39, pp. 1471–1482. https://doi.org/10.1002/nag.2366

29. Bulat, A.F., Lukinov V.V., and Bezruchko, K.A. (2017), *Umovy formuvannia hazovykh pastok u vuhlenosnykh vidkladakh* [Conditions for the formation of gas traps in coal-bearing deposits], Naukova dumka, Kyiv, Ukraine.

30. Shvets, V.B., Boiko, I.P. and Vynnykov, Yu.L. (2012), *Mekhanika gruntiv. Osnovy ta fundamenty: Pidruchnyk* [Soil Mechanics. Fundamentals and Foundations: Textbook], Porohy, Dnipropetrovsk, Ukraine.

31. Rust, W. (2012), *Non-Linear Finite Element Analysis in Structural Mechanics*, Springer, Hannover, Germany.

32. Zienkiewicz, O.C., Taylor, R.L. and Zhu, J.Z. (2013), *The Finite Element Method: Its Basis and Fundamentals*, Butterworth-Heinemann, Amsterdam, Netherlands.

33. Kaya, A., Karaman, K. and Bulut, F. (2017), "Geotechnical investigations and remediation design for failure of tunnel portal section: a case study in northern Turkey", *Journal of Mountain Science*, no. 14(6), pp. 1140–1160. https://doi.org/10.1007/s11629-016-4267-x

About the authors

Krukovska Viktoriia, Doctor of Technical Sciences (D. Sc), Senior Researcher, Senior Researcher in Department of Dynamic Manifestations of Rock Pressure, M.S. Poliakov Institute of Geotechnical Mechanics of the National Academy of Sciences of Ukraine (IGTM, NASU), Dnipro, Ukraine, vikakrukk@gmail.com ***(Corresponding author)***, ORCID ***0000-0002-7817-4022***

Krukovskyi Oleksandr, Corresponding Member of NAS of Ukraine, Doctor of Technical Sciences (D. Sc), Deputy Director of the Institute, M.S. Poliakov Institute of Geotechnical Mechanics of the National Academy of Sciences of Ukraine (IGTM, NASU), Dnipro, Ukraine, igtm@ukr.net, ORCID ***0000-0002-2659-5095***

Vynohradov Yurii, Candidate of Technical Sciences (Ph.D), Researcher in Department of Control of Rocks State, Branch for Physics of Mining Processes of the M.S. Poliakov Institute of Geotechnical Mechanics of the National Academy of Sciences of Ukraine, Dnipro, Ukraine, my_pochta_1r@ukr.net, ORCID ***0000-0002-4823-6480***

ФІЛЬТРАЦІЯ ПІДЗЕМНИХ ВОД ДО ТУНЕЛЮ, ЩО СПОРУДЖУЄТЬСЯ В ТРІЩИНУВАТИХ СКАЛЬНИХ ПОРОДАХ

Круковська В.В., Круковський О.П., Виноградов Ю.О.

Анотація. Ґрунтові води є одним із факторів, що загрожують стабільності та безпеці вже під час будівництва тунелів, особливо з огляду на те, що за непередбачуваних обставин можуть статися тривалі затримки у встановленні кріплення і герметизації підземного об'єкту. Тому в роботі розглядається фільтрація підземних вод до тунелю в період часу між виїмкою породи і установкою початкового кріплення.

Було досліджено вплив ступеню порушеності порід на їх деформування і фільтрацію води та зроблено наступні виводи. Зі зниженням міцності породи площа зони підвищеної різнокомпонентності поля напружень навколо тунелю зменшується. В інтенсивно тріщинуватому масиві відбувається крихке руйнування приконтурних порід шляхом розділення на блоки, в зонах інтенсивної каолінізації – пластичне руйнування за рахунок зволоженого каолініту. В цих випадках спостерігаються і найбільші нормальні переміщення контуру тунелю.

Рівень проникності визначає інтенсивність фільтраційного процесу, тому тиск води в тріщинному просторі непорушених скальних порід практично не змінюється з часом. В момент часу t = 8 діб, в нерівномірно і сильно тріщинуватих породах тиск води помітно нижчий в приконтурній області, а в інтенсивно тріщинуватому граніті навколо тунелю утворено широку область, де тиск є значно меншим за гідростатичний. Тобто за умови високої проникності скельного масиву має місце значний гідравлічний вплив незакріпленого тунелю на природний стан підземних вод, що у подальшому загрожує зниженням рівня ґрунтових вод і може вплинути на водозабори, природні джерела, осушення ґрунтів та осідання ґрунту через втрату порового тиску.

Тому при спорудженні тунелів треба мінімізувати час встановлення тимчасового кріплення і герметизації контуру, особливо в інтенсивно порушених зонах. Крім того, оскільки не завжди можливо передбачити усі геологічні порушення і структури по трасі спорудження підземного об'єкту, при проектуванні кріплення важливо передбачити можливість ситуативного посилення кріплення, у випадку перетину непрогнозованого геологічного порушення.

Ключові слова: тунель, тріщинуватий породний масив, фільтрація ґрунтових вод, гідравлічний вплив незакріпленого тунелю, чисельне моделювання.